

Glauber gluons in pion-induced Drell-Yan processes revisited

Hsiang-nan Li*

Institute of Physics, Academia Sinica, Taipei, Taiwan 115, Republic of China

We reanalyze the anomalous angular distribution of lepton pairs produced in a pion-induced Drell-Yan process by taking into account the Glauber gluon effect in the k_T factorization theorem. Compared to the previous study, we adopt the realistic parton distribution functions (PDFs) for a proton from the CTEQ and for a pion from the xFitter, include the QCD evolutions of the strong coupling and the PDFs, and integrate the differential cross section over the kinematic regions for the NA10, E615 and COMPASS experiments. These improvements then allow rigorous confrontations of theoretical results with the data. It is shown that the lepton angular distribution and the violation of the Lam-Tung relation measured in all the above experiments can be well accommodated with a single Glauber phase. We illustrate the Glauber effect in the geometric picture for a Drell-Yan process, and its distinction from the conventional Boer-Mulders mechanism. The observables are pointed out, which can be used to discriminate the two proposals, when data become more precise.

PACS numbers:

The anomalous angular distribution of lepton pairs produced in a pion-induced Drell-Yan process has been a long-standing puzzle. To explain this anomaly, we write the relevant differential cross section as [1, 2]

$$\frac{1}{\sigma} \frac{d\sigma}{d\Omega} = \frac{3}{4\pi} \frac{1}{\lambda + 3} \left(1 + \lambda \cos^2 \theta + \mu \sin 2\theta \cos \phi + \frac{\nu}{2} \sin^2 \theta \cos 2\phi \right), \quad (1)$$

with $d\Omega \equiv d\cos\theta d\phi$, where θ (ϕ) is the polar (azimuthal) angle of one of the leptons in the Collins-Soper (CS) frame [3]. We consider the process at an intermediate lepton-pair invariant mass Q , to which the virtual photon contribution dominates over the Z boson one. The coefficients λ and ν are supposed to obey the Lam-Tung (LT) relation $\delta \equiv 2\nu + \lambda - 1 = 0$ [2] at a low lepton-pair transverse momentum q_T , that has been shown to hold largely under perturbative corrections [4, 5] and under parton-transverse-momentum and soft-gluon effects [6, 7]. Though the LT relation was verified experimentally in the proton-proton and proton-deuteron Drell-Yan processes [8], significant violation in the pion-induced ones was observed by the NA10 [9] and E615 [10], and recently by the COMPASS [11]: the substantial deviation from $\delta = 0$ clearly increases with q_T .

The above anomaly has stimulated extensive theoretical investigations on its origin, which mainly resort to nonperturbative mechanisms [12–22]. For example, the vacuum effect proposed in [12, 13] causes the transverse-spin correlation between colliding partons, and the Boer-Mulders (BM) functions [16] introduce the spin-transverse-momentum correlation of a parton in an unpolarized hadron. As pointed out in [19], the vacuum effect is flavor-blind, so it is difficult to differentiate the pion-proton and proton-proton processes. The proposal based on the BM functions can differentiate these two processes, because a colliding anti-quark is a valence parton in a pion, but a sea parton in a proton [23]. Note that the BM functions resolve the violation of the LT relation by increasing the coefficient ν in Eq. (1) without changing λ . Our resolution [21] relies on infrared Glauber gluons appearing in the k_T factorization theorem for complicated QCD processes [24, 25], whose effect might be significant due to the unique role of a pion as a Nambu-Goldstone (NG) boson and a $q\bar{q}$ bound state simultaneously [26]. The Glauber effect can modify the perturbative results of both λ and ν , and account for the LT violation observed in the pion-induced Drell-Yan process. An anti-proton is not a NG boson, so its associated Glauber effect is expected to be weak, and the LT relation should be respected. It was thus suggested that examining the LT relation in a proton-anti-proton Drell-Yan process at low q_T could discriminate the two mechanisms [21]: if violation is (not) observed, our (BM) proposal is irrelevant.

In this paper we will elaborate the proposal based on the Glauber gluon effect, and confront it with the data, especially the preliminary COMPASS data [11], for the pion-induced Drell-Yan process. The purpose of our previous study [21] was to demonstrate the phenomenological impacts of the Glauber effect, and to estimate the LT violation at fixed rapidity y and lepton-pair invariant mass Q . This is the reason why naive models for the parton distribution functions (PDFs) of a proton and a pion were employed in the factorization formulas to evaluate the angular coefficients. Hence, the theoretical results presented in [21] might not be compared with the data seriously. In the present work we will adopt the realistic PDFs for a proton from the CTEQ (CT18) [27] and for a pion from the xFitter [28]. The latter are similar to those from the JAM [29]. We will also implement the QCD evolutions of the strong coupling α_s in the hard kernels involved in the factorization formulas and of the PDFs, and integrate the differential

*Electronic address: hnli@phys.sinica.edu.tw

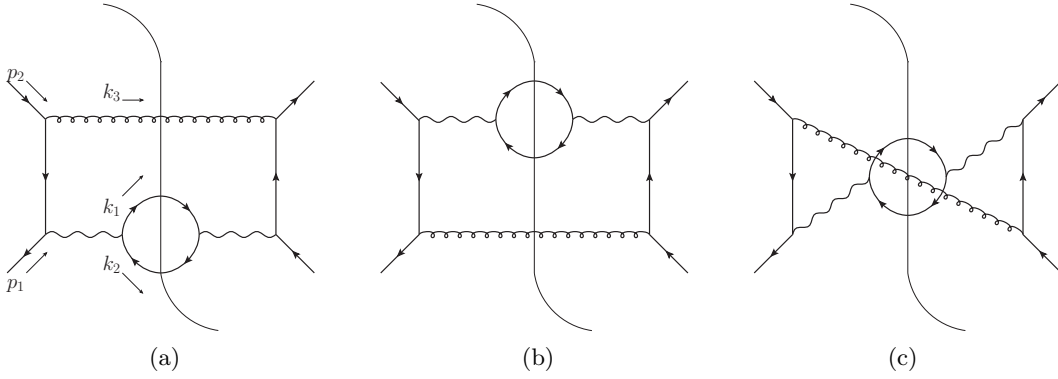


FIG. 1: LO diagrams for $\bar{q}(p_1) + q(p_2) \rightarrow \ell^-(k_1) + \ell^+(k_2) + g(k_3)$ in the pion-proton Drell-Yan process, where the variables in the parentheses label the parton momenta.

cross sections over the kinematic regions considered in different experiments. As observed in [30, 31], the theoretical outcomes for the three angular coefficients are sensitive to the variation of Q actually. The above improvements then allow rigorous confrontations of our results for low q_T spectra with the data. It will be shown that the Glauber effect enhances both λ and ν in the perturbation theory [32, 33], and leads to a better agreement with the NA10 data [9]. The perturbative results for μ remain small under the Glauber effect, and match the data within experimental uncertainties. We then make predictions for the E615 [10] and COMPASS [11] measurements with the same Glauber effect, and confirm that the observed LT violation is also accommodated.

It has been found [33] that the contribution to the aforementioned Drell-Yan processes from the $q\bar{q}$ (quark-anti-quark) channel is more important than from the qg (quark-gluon) channel. For instance, the former contributes more than 80% of the total cross section for the COMPASS kinematics [30]. This observation is reasonable, since the region with large parton momentum fractions dominates in fixed-target experiments, where gluonic partons have smaller distributions. Besides, currently available data are not precise enough for determining the sea and gluon distributions unambiguously [28]. It has been verified that the coefficients λ and ν are rather insensitive to resummation effects [32] and to next-to-leading-order (NLO) corrections at small $q_T \leq 3$ GeV [30, 32], which we are focusing on. Therefore, we will confine ourselves to the leading-order (LO), i.e., $O(\alpha_s)$ $q\bar{q}$ contribution without the resummation in the investigation below. Note that tungsten was used in all the experiments involving pions [9–11], but we will not take into account nuclear effects as in [32]. The LO parton-level diagrams for the scattering $\bar{q}(p_1) + q(p_2) \rightarrow \ell^-(k_1) + \ell^+(k_2) + g(k_3)$ in the pion-proton Drell-Yan process, where the variables in the parentheses label the parton momenta with $k_3 = p_1 + p_2 - k_1 - k_2$, are displayed in Fig. 1. The momentum p_1 (p_2) with the dominant plus (minus) component is carried by the valence anti-quark (quark) in the pion (proton). The explicit expressions of the corresponding hard kernels are referred to [7, 34–38].

We first briefly review the appearance of infrared Glauber divergences in radiative corrections to Fig. 1. It is obvious that the low q_T spectra of lepton pair productions in a Drell-Yan process meet the necessary conditions for the existence of Glauber gluons: the k_T factorization theorem is the appropriate theoretical framework for the low q_T spectra, in which the dependence on parton transverse momenta should be kept; a final-state parton is required to balance the lepton-pair q_T , so at least three partons participate the hard scattering; the lepton-pair momentum $q = k_1 + k_2$ is restricted in a finite phase space, such that the final-state parton is not fully inclusive in kinematics, and the Glauber divergences in various diagrams do not cancel exactly. We stress that a final-state parton is needed to help balance q_T , as q_T is about few GeV, the region where the LT violation is significant. The intrinsic transverse momenta of the initial-state partons alone are insufficient to sustain such q_T . According to the elucidation in [21, 24, 25, 39], radiative gluons emitted by a spectator line in the pion (like a rung gluon that can be exchanged between the two anti-quarks of the momentum p_1 in Fig. 1), and attaching to lines in other subprocesses produce Glauber divergences. For the diagrams in Fig. 1, the Glauber divergences are extracted from the attachments to the quark of the momentum p_2 in the proton, to the gluon of the momentum k_3 , and to the vertical quark lines [39]. Note that a Glauber gluon, different from an ordinary soft gluon, gives rise to an imaginary infrared logarithm. To get a real cross section, at least two Glauber gluons are present, which may be located on the same side or on the opposite sides of the final-state cut. It has been shown that the infrared divergences from these two types of gluon allocations do not cancel exactly in the k_T factorization theorem [25], and that the imaginary Glauber logarithms can be factorized into a universal nonperturbative phase factor to all orders in α_s at low q_T [39].

The transverse momentum l_T of a Glauber gluon flows through the parton-level hard kernels represented by the

two vertical quark lines in Fig. 1 [39]. The two vertical quarks in Fig. 1(a) have small invariant masses in the positive rapidity region of the lepton pair, and those in Fig. 1(b) have small invariant masses in the negative rapidity region. However, the two vertical quarks in Fig. 1(c) cannot have small invariant masses simultaneously: the quark on the left-hand (right-hand) side of the final-state cut has a small (large) invariant mass, as the lepton pair is produced with positive rapidity. This difference in the hard kernels, as the differential cross section is integrated over the rapidity, renders the net Glauber effect from the two sides of the final-state cut suppressed for Fig. 1(c) compared to those for Figs. 1(a) and 1(b). To elaborate the above statement, we quote the factorization formula in the impact-parameter space for a Drell-Yan process with Glauber gluon exchanges [39]

$$\int d^2b_l d^2b_r d^2b'_l d^2b'_r e^{-iS(\mathbf{b}_l)} H(\mathbf{b}_l - \mathbf{b}'_l, \mathbf{b}_r - \mathbf{b}'_r) e^{iS(\mathbf{b}_r)} \Phi_\pi(\mathbf{b}'_l, \mathbf{b}'_r) e^{-i\mathbf{q}_T \cdot (\mathbf{b}_l - \mathbf{b}_r - \mathbf{b}'_l + \mathbf{b}'_r)} \dots, \quad (2)$$

where only the relevant factors are shown explicitly, and the exponentials $e^{\pm iS}$ organize the Glauber gluons to all orders in α_s . In the presence of the Glauber gluons that carry transverse momenta, both the Fourier-transformed hard kernel H and transverse-momentum-dependent (TMD) pion PDF Φ_π depend on two impact parameters. That is, the partons on the left-hand (labelled by the subscripts l) and right-hand (labelled by the subscripts r) sides of the final-state cut have different transverse coordinates.

It is easy to see from Eq. (2) that both the arguments $\mathbf{b}_l - \mathbf{b}'_l$ and $\mathbf{b}_r - \mathbf{b}'_r$ can be large, when the two vertical quarks have small invariant masses as they do in Figs. 1(a) and 1(b). Namely, \mathbf{b}_l (\mathbf{b}_r) is different from \mathbf{b}'_l (\mathbf{b}'_r), and takes a value in a wide range, so there is no strong cancellation between the Glauber factors $e^{-iS(\mathbf{b}_l)}$ and $e^{iS(\mathbf{b}_r)}$ from the two sides of the final-state cut. When one of the vertical quarks, say, the one on the right-hand side of the final-state cut has a large invariant mass, the region with small $\mathbf{b}_r - \mathbf{b}'_r$, i.e., with $\mathbf{b}_r \approx \mathbf{b}'_r$ dominates. For a finite q_T of order 1 GeV, the Fourier factor in Eq. (2), $\exp[-i\mathbf{q}_T \cdot (\mathbf{b}_l - \mathbf{b}_r - \mathbf{b}'_l + \mathbf{b}'_r)] \approx \exp[-i\mathbf{q}_T \cdot (\mathbf{b}_l - \mathbf{b}'_l)]$, enforces the condition that \mathbf{b}_l cannot be very different from \mathbf{b}'_l . It turns out that both \mathbf{b}_l and \mathbf{b}_r are restricted in the support of \mathbf{b}'_l and \mathbf{b}'_r for $\Phi_\pi(\mathbf{b}'_l, \mathbf{b}'_r)$ defined by the transverse extent of the pion. The cancellation between $e^{-iS(\mathbf{b}_l)}$ and $e^{iS(\mathbf{b}_r)}$ then becomes stronger, explaining why the net Glauber effect is minor for Fig. 1(c). Below we will neglect the Glauber effect on Fig. 1(c), and assume that Figs. 1(a) and 1(b) acquire an additional factor $\cos S$ [21]. The Glauber phase S is proportional to the product of α_s and an infrared logarithm, if computed in the perturbation theory. The expansion of the Glauber factor $\cos S$ in powers of α_s reflects the fact that an odd number of Glauber gluons does not contribute to a real cross section. Because the Glauber phase is of nonperturbative origin, and its explicit expression is unknown, we simply treat S as a constant, which parametrizes the Glauber effect averaged over the impact parameters, i.e., over the internal transverse momenta. The complexity of the analysis is thus greatly reduced by avoiding the lengthy convolution in Eq. (2). The simplified factorization formulas with the average Glauber phase S are derived in detail in the Appendix.

It has been pointed out [40] that a Glauber factor, despite being universal once the k_T factorization is established, generates different effects in different processes. The reason is that a Glauber factor makes its impact through the convolution with other subprocesses, including TMD hadron wave functions. As demonstrated in [40], the pion (ρ meson) TMD wave function with a weak (strong) falloff in a parton transverse momentum leads to significant (moderate) Glauber effects on two-body hadronic B meson decays. This observation is consistent with the dual role of a pion as a massless NG boson and as a $q\bar{q}$ bound state, which requires a tighter spatial distribution for its leading Fock state. The Glauber effect has been introduced to resolve several puzzling data in two-body hadronic heavy flavor decays into pions, such as the abnormally large $B^0 \rightarrow \pi^0 \pi^0$ and $\pi^0 \rho^0$ branching ratios [41–43], the very different direct CP asymmetries in the $B^+ \rightarrow \pi^0 K^+$ and $B^0 \rightarrow \pi^- K^+$ decays [44, 45], and the difference between the $D^0 \rightarrow \pi^+ \pi^-$ and $K^+ K^+$ branching ratios that exceeds the expected SU(3) symmetry breaking [46–48]. It has been elaborated recently that the data of the $D \rightarrow \pi\pi$ and πK branching ratios reveal prominent Glauber effects [48].

We start with the differential cross section for the pion-proton Drell-Yan process

$$\begin{aligned} \frac{d\sigma}{dQ^2 dy dq_T^2 d\Omega} &= \frac{N}{s^2} \left[H_0(Q^2, y, q_T^2) + H_\lambda(Q^2, y, q_T^2) \cos^2 \theta + H_\mu(Q^2, y, q_T^2) \sin 2\theta \cos \phi \right. \\ &\quad \left. + \frac{1}{2} H_\nu(Q^2, y, q_T^2) \sin^2 \theta \cos 2\phi \right], \end{aligned} \quad (3)$$

where the normalization constant N is irrelevant to the evaluations of the angular coefficients, and s is the center-of-mass energy squared. The functions H_i , $i = 0, \lambda, \mu$ and ν , are written as the convolutions of the hard kernels \hat{H}_i

with the pion PDF ϕ_π and the proton PDF ϕ_P at the scale $\mu = Q$,

$$H_i(Q^2, y, q_T^2) = \frac{\alpha_s(Q^2)}{Q^2} \int dx_1 dx_2 \phi_\pi(x_1, Q^2) \hat{H}_i(x_1, x_2, Q^2, y, q_T^2) \phi_P(x_2, Q^2) \times \delta \left(x_1 x_2 - (x_1 e^{-y} + x_2 e^y) \frac{\sqrt{Q^2 + q_T^2}}{\sqrt{s}} + \frac{Q^2}{s} \right). \quad (4)$$

The δ function, arising from the on-shell condition $k_3^2 = 0$, specifies the relation between the parton momentum fractions x_1 and x_2 . It has been checked that the alternative choice $\mu = \sqrt{Q^2 + q_T^2}$ yields very similar results even at LO [32]. The angular coefficients in Eq. (1) and the LT violation δ are defined by

$$\lambda, \mu, \nu, \delta = \frac{\int dQ^2 dy H_{\lambda, \mu, \nu, \delta}(Q^2, y, q_T^2)}{\int dQ^2 dy H_0(Q^2, y, q_T^2)}, \quad (5)$$

where the factorization formula for H_δ is similar to Eq. (4) with the hard kernel \hat{H}_δ . We point out that ν is more sensitive to the changes of PDFs than λ , and that μ is equal to zero, when the pion and proton PDFs have the same functional form [21].

To present the expressions of the LO hard kernels \hat{H}_i , we first choose the parton and lepton momenta in the CS frame as

$$\begin{aligned} p_1 &= E_1(1, -\sin \theta_1, 0, \cos \theta_1), & p_2 &= E_2(1, -\sin \theta_1, 0, -\cos \theta_1), \\ k_1 &= k(1, \sin \theta \cos \phi, \sin \theta \sin \phi, \cos \theta), & k_2 &= k(1, -\sin \theta \cos \phi, -\sin \theta \sin \phi, -\cos \theta), \end{aligned} \quad (6)$$

where E_1 and E_2 are the parton energies, k is the lepton energy, and θ_1 is the angle between the momentum \mathbf{p}_1 and the z axis. In terms of the kinematic variables in Eq. (6), \hat{H}_i from the $q\bar{q}$ channel modified by the Glauber factor $\cos S$ read

$$\begin{aligned} \hat{H}_0 &= \left(\frac{E_1}{E_2} + \frac{E_2}{E_1} \right) \left(\frac{1}{\sin^2 \theta_1} + \frac{1}{2} \right) \\ &+ (\cos S - 1) \left[\left(\frac{2E_1 E_2}{k^2} \cos^2 \theta_1 - \frac{E_1}{E_2} - \frac{E_2}{E_1} \right) \left(\frac{1}{\sin^2 \theta_1} - \frac{1}{2} \right) + \left(\frac{k}{E_1} + \frac{k}{E_2} - 2 \right) \frac{2}{\sin^2 \theta_1} \right] \end{aligned} \quad (7)$$

$$\begin{aligned} \hat{H}_\lambda &= \left(\frac{E_1}{E_2} + \frac{E_2}{E_1} \right) \left(\cot^2 \theta_1 - \frac{1}{2} \right) \\ &+ (\cos S - 1) \left[\left(\frac{E_1}{E_2} + \frac{E_2}{E_1} - 2 \right) \left(\cot^2 \theta_1 - \frac{1}{2} \right) + \frac{E_1 E_2}{k^2} \cos^2 \theta_1 - 1 \right], \end{aligned} \quad (8)$$

$$\hat{H}_\mu = \left(\frac{E_2}{E_1} - \frac{E_1}{E_2} \right) \cot \theta_1 + (\cos S - 1) \left(\frac{E_1 - E_2}{k} + \frac{E_2}{E_1} - \frac{E_1}{E_2} \right) \cot \theta_1, \quad (9)$$

$$\hat{H}_\nu = \left(\frac{E_1}{E_2} + \frac{E_2}{E_1} \right) - (\cos S - 1) \left(\frac{2E_1 E_2}{k^2} \cos^2 \theta_1 - \frac{E_1}{E_2} - \frac{E_2}{E_1} \right), \quad (10)$$

$$\hat{H}_\delta = \frac{2(\cos S - 1)}{\sin^2 \theta_1} \left[\frac{E_1 - k}{E_2} + \frac{E_2 - k}{E_1} - \left(\frac{E_1 E_2}{k^2} \cos^2 \theta_1 - 1 \right) (1 + \sin^2 \theta_1) \right], \quad (11)$$

where those pieces multiplied by $\cos S - 1$ arise from Figs. 1(a) and 1(b). It is seen that the hard kernel \hat{H}_δ for LT violation δ vanishes as $S = 0$. Compared to [21], an overall factor $1/\sin^2 \theta_1$, that depends on the lepton-pair invariant mass Q , has been included. This factor was neglected before, since it cancels in the ratios for defining the angular coefficients at fixed Q . Here we will integrate the differential cross section over kinematic variables in order to confront our results with the data rigorously.

We then transform the kinematic variables E_1 , E_2 , k , and θ_1 in the CS frame to those in the center-of-mass frame of the colliding hadrons via [21]

$$k = \frac{Q}{2}, \quad \sin \theta_1 = \frac{q_T}{\sqrt{Q^2 + q_T^2}}, \quad E_1 = \frac{e^{-y}}{\cos \theta_1} x_1 P_1^0, \quad E_2 = \frac{e^y}{\cos \theta_1} x_2 P_2^0, \quad (12)$$

with the pion and proton energies $P_1^0 = P_2^0 = \sqrt{s}/2$, and obtain the hard kernels $\hat{H}_i(x_1, x_2, Q^2, y, q_T^2)$. It is found that $\sin \theta_1$ is proportional to the lepton-pair transverse momentum q_T , i.e., to the boost of the CS frame relative to the

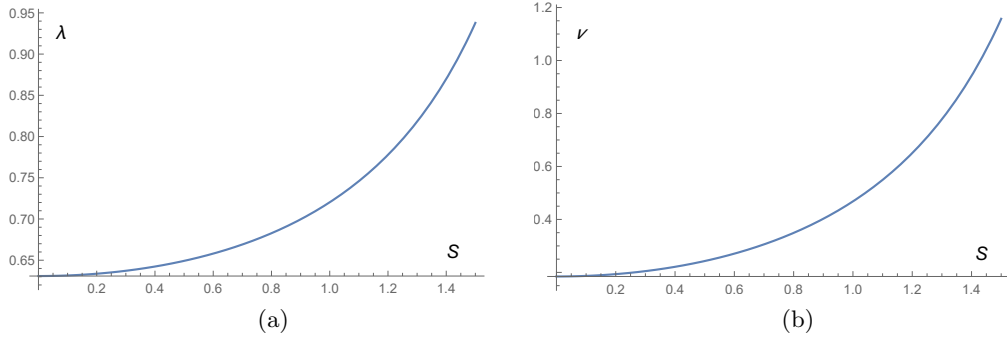


FIG. 2: Dependencies of the angular coefficients (a) λ and (b) ν on the Glauber phase S for the pion beam energy $E_\pi = 194$ GeV and the lepton-pair transverse momentum $q_T = 2.5$ GeV with the cuts in Eq. (15).

center-of-mass frame. The constraint on the gluon energy $k_3^0 > 0$ together with the on-shell condition $k_3^2 = 0$ favors the region of large momentum fractions,

$$\frac{e^y \sqrt{Q^2 + q_T^2} - Q^2/\sqrt{s}}{\sqrt{s} - e^{-y} \sqrt{Q^2 + q_T^2}} \leq x_1 \leq 1, \quad (13)$$

for an intermediate Q , which dominates in fixed-target experiments.

We calculate the angular coefficients to be compared with the NA10 data [9], adopting the PDFs for a proton from the CT18 [27] and for a pion from the xFitter [28]. The integrations in Eq. (5) are performed over the range $Q \geq 4$ GeV for the pion beam energy $E_\pi = 286$ GeV, over $Q \geq 4.05$ GeV for $E_\pi = 194$ GeV, and over $Q \geq 4$ GeV for $E_\pi = 140$ GeV with the bottomonium region $8.5 \text{ GeV} \leq Q \leq 11 \text{ GeV}$ being excluded [32]. The cut $0 \leq x_\pi \leq 0.7$ is also implemented with

$$x_\pi = \frac{1}{2} \left(x_F + \sqrt{x_F^2 + \frac{4Q^2}{s}} \right), \quad (14)$$

x_F being the Feynman variable. The variable x_π corresponds to the parton momentum fraction x_1 , and x_F ($\sqrt{x_F^2 + 4Q^2/s}$) is proportional to the longitudinal momentum (energy) of the lepton pair in the limit $k_3 \rightarrow 0$ in the center-of-mass frame of the colliding hadrons. The physical ranges of Q and y for a given q_T are those, in which x_1 and x_2 take values between 0 and 1. The combination of the above kinematic constraints leads to the ranges

$$\begin{aligned} \frac{1}{2} (b - \sqrt{b^2 - 4}) &\leq e^y \leq \frac{1}{2} (a + \sqrt{a^2 + 4}), \quad Q^2 \leq 0.7s \sqrt{1 - \frac{4q_T^2}{(1 - 0.7^2)s}} \\ \frac{1}{2} (b - \sqrt{b^2 - 4}) &\leq e^y \leq \frac{1}{2} (b + \sqrt{b^2 - 4}), \quad 0.7s \sqrt{1 - \frac{4q_T^2}{(1 - 0.7^2)s}} \leq Q^2 \leq s - 2\sqrt{s}q_T, \\ a &= \frac{0.7^2 s - Q^2}{0.7\sqrt{s(Q^2 + q_T^2)}}, \quad b = \sqrt{\frac{s}{Q^2 + q_T^2}} \left(1 + \frac{Q^2}{s} \right). \end{aligned} \quad (15)$$

Equation (15) implies that the allowed range of y shrinks with Q^2 , and $y \rightarrow 0$ as Q^2 approaches to its upper bound $s - 2\sqrt{s}q_T$.

The dependencies of the angular coefficients λ and ν on the Glauber phase S for the pion beam energy $E_\pi = 194$ GeV and the lepton-pair transverse momentum $q_T = 2.5$ GeV under the cuts in Eq. (15) are displayed in Fig. 2. It is found that the values of λ and ν at $S = 0$, i.e., the perturbative results without the Glauber effect, reproduce those in [30, 32]. Namely, the simplification made in our calculation, i.e., considering only the LO $q\bar{q}$ channel is justified. It is interesting to see that the Glauber effect enhances both λ and ν , and the deviation from the LT relation $2\nu + \lambda - 1 = 0$ is then induced. As emphasized before, this feature differentiates our resolution to the LT violation from the one based on the BM functions, which increases only ν . Therefore, separate comparisons of theoretical predictions with future precise data of λ and ν is likely to discriminate the two proposals. We observe that our results of ν are more sensitive to the variation of the Glauber phase than those of λ , and that the NA10 data for ν are more precise than for λ (and also more precise than the E615 and COMPASS data). We thus fix $S = 0.8$ by collating Fig. 2(b) and the

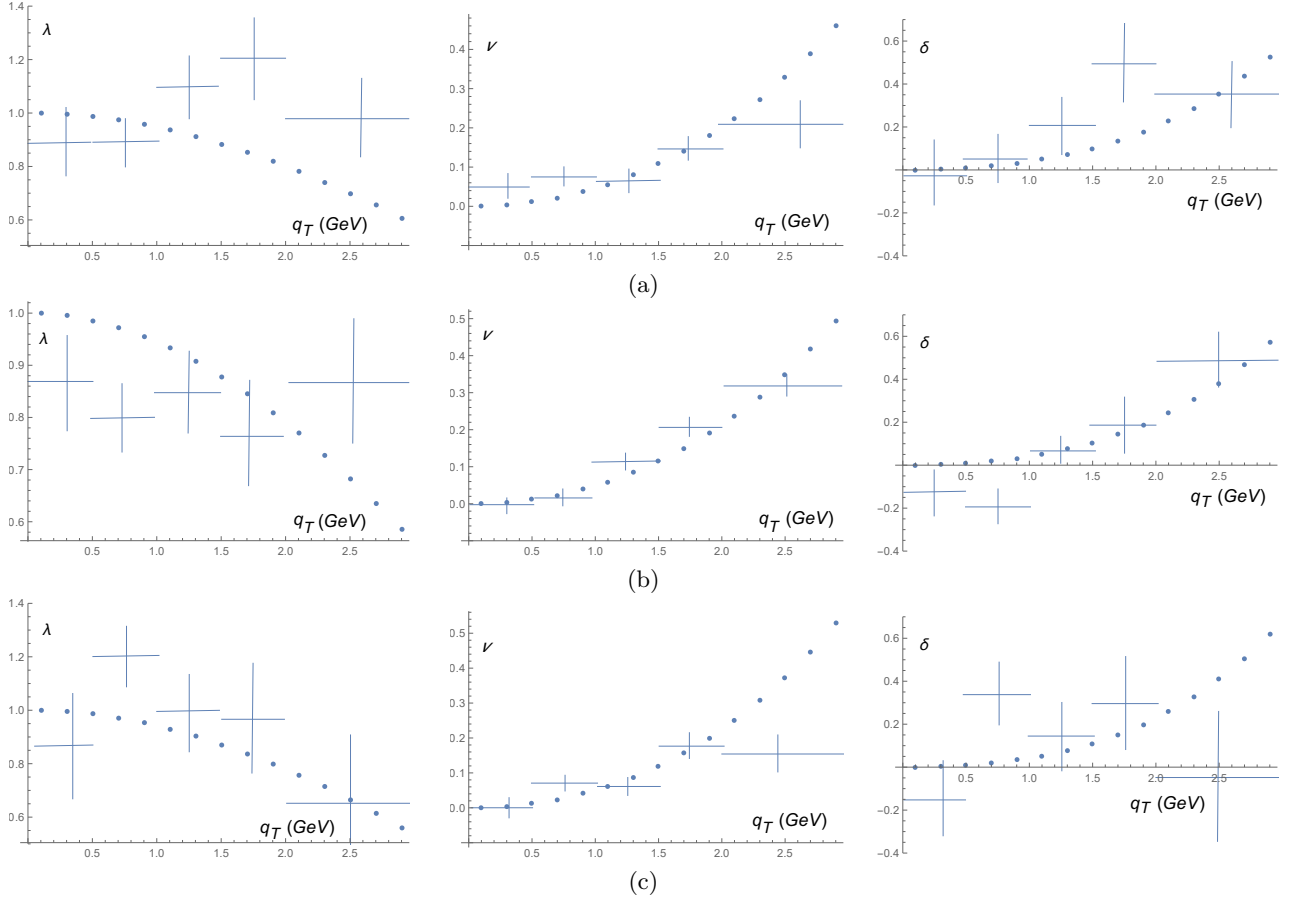


FIG. 3: Dependencies of λ , ν , and the LT violation $\delta \equiv 2\nu + \lambda - 1$ on the lepton-pair transverse momentum q_T , and their comparisons with the NA10 data [9] for the pion beam energies (a) $E_\pi = 286$ GeV, (b) $E_\pi = 194$ GeV, and (c) $E_\pi = 140$ GeV.

NA10 data for ν at $E_\pi = 194$ GeV and $q_T = 2.5$ GeV, and employ this single input to make predictions for all other quantities. With $S = 0.8$, the perturbative values of λ are enhanced by 10%, which is not as strong as obtained in our previous naive estimate [21], and those of ν are enhanced by a factor of 2. We simply vary the Glauber phase to $S = 0.7$ and $S = 0.9$ to assess the theoretical uncertainties, which are about 5% for λ and 15% for ν . It is noticed that the angular coefficient μ remains tiny [21]: it takes the value $\mu = -0.028$ for $S = 0.8$ and $q_T = 2.5$ GeV, which is consistent with the NA10 data, and much smaller than the experimental errors. We will not present the results of μ hereafter.

The changes of the angular coefficients λ and ν , and the violation $\delta \equiv 2\nu + \lambda - 1$ of the LT relation with the lepton-pair transverse momentum q_T for the Glauber phase $S = 0.8$ under Eq. (15) are exhibited in Fig. 3. We focus on the low $q_T \leq 3$ GeV region, for which the k_T factorization theorem is more appropriate, and the Glauber effect is expected to be significant. Note that the curve of ν in Fig. 3(b) will go below the data for $E_\pi = 194$ GeV, if S is set to 0.7, and those will go above the data for $E_\pi = 286$ GeV and 140 GeV, if S is set to 0.9. This check supports our choice $S = 0.8$, which improves the overall agreement with the NA10 data [9] of λ and ν for the three different pion beam energies E_π as indicated in Fig. 3. The decrease of λ with q_T is moderated a bit and the increase of ν with q_T is strengthened by the Glauber effect, such that the measured LT violations δ are well accommodated. We point out that all the functions $H_i(Q^2, y, q_T^2)$ decrease with q_T , but $H_\nu(Q^2, y, q_T^2)$ decreases more slowly under the Glauber effect, explaining the large enhancement of ν . This feature will be illustrated in the geometric picture near the end of this paper. We have confirmed that the perturbative results for δ , corresponding to $S = 0$, vanish at LO, and coincide with the horizontal axes in Fig. 3. The NLO results for δ , being negative and nearly zero with magnitudes smaller than 0.1 in the region $q_T \leq 3$ GeV [30], still deviate from the data obviously. We remind that the ascent of the curves for δ in Fig. 3 should not extend to the high q_T region, where the collinear factorization holds, and the Glauber effect is supposed to diminish. In fact, the LT violation $\delta < 0$ with an opposite sign has been observed at high q_T of Z boson production in proton-proton collisions [49]. As to the dependence on the pion beam energy, we

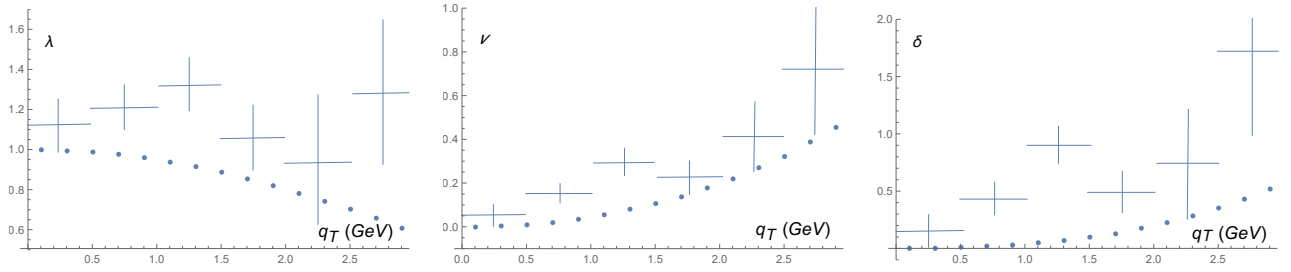


FIG. 4: Dependencies of λ , ν , and the LT violation δ on the lepton-pair transverse momentum q_T , and their comparisons with the E615 data [10] for the pion beam energy $E_\pi = 252$ GeV.

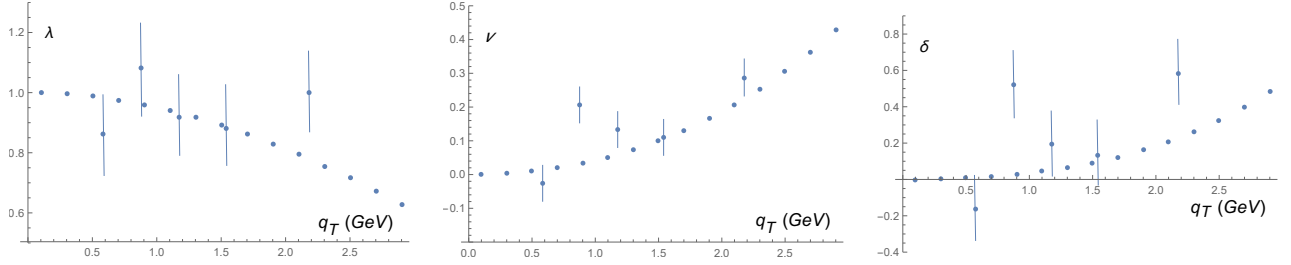


FIG. 5: Dependencies of λ , ν , and the LT violation δ on the lepton-pair transverse momentum q_T , and their comparisons with the COMPASS data [11] for the pion beam energy $E_\pi = 190$ GeV.

find that the results of λ (ν) increase (decrease) with E_π for fixed q_T , so those of δ decrease with E_π .

The kinematic cuts $4.05 \leq Q \leq 8.55$ GeV, $0.2 \leq x_\pi \leq 1$ and $0 \leq x_F \leq 1$ were implemented in the E615 experiment with the pion beam energy $E_\pi = 252$ GeV [10]. We perform the integrations in Eq. (5) over the ranges of y and Q accordingly,

$$\begin{aligned} \frac{1}{2} \left(c + \sqrt{c^2 + 4} \right) &\leq e^y \leq \frac{1}{2} \left(b + \sqrt{b^2 - 4} \right), \quad \text{as } Q^2 \leq 0.2^2 s, \\ 1 \leq e^y &\leq \frac{1}{2} \left(b + \sqrt{b^2 - 4} \right), \quad \text{as } Q^2 > 0.2^2 s, \\ c &= \frac{0.2^2 s - Q^2}{0.2 \sqrt{s(Q^2 + q_T^2)}}. \end{aligned} \quad (16)$$

The predicted q_T spectra of the angular coefficients λ and ν , and the LT violation δ for the Glauber phase $S = 0.8$ under Eq. (16) are shown in Fig. 4, whose behaviors are close to those in Fig. 3. The discussions of the Glauber effect on those q_T spectra also proceed similarly. Our predictions for ν and δ are slightly lower than the E615 data [10], but the consistency is still satisfactory, after the sizable experimental errors are considered. In particular, the deviation from the LT relation, i.e., from the horizontal axis in the third plot, is roughly accounted for by the Glauber effect.

At last, we make predictions for the COMPASS measurements with the pion beam energy $E_\pi = 190$ GeV. The corresponding cuts $4.3 \text{ GeV} \leq Q \leq 8.5 \text{ GeV}$ and $x_F \geq -0.1$ [11] lead to the range of y ,

$$\frac{1}{2} \left(d + \sqrt{d^2 + 4} \right) \leq e^y \leq \frac{1}{2} \left(b + \sqrt{b^2 - 4} \right), \quad d = \frac{-0.1 \sqrt{s}}{\sqrt{Q^2 + q_T^2}}. \quad (17)$$

The dependencies of λ , ν and δ on q_T , displayed in Fig. 5, are similar to those derived in the previous cases. A careful look at Figs. 3(b) and 5 with the approximately equal pion beam energies reveals that the values of λ (ν) in the former are lower (higher) than in the latter. This difference may be attributed to the slightly lower Q region that the NA10 measurements have probed. The behaviors of these angular coefficients in various bins of Q , investigated in [30], concur the above tendency. Though the preliminary COMPASS data [11] are not yet precise enough, the general features remain the same: the decrease (increase) of λ (ν) with q_T is milder (stronger) than expected by the perturbation theory [30], and the observed δ , i.e., the deviation from the horizontal axis in the third plot, is significant.

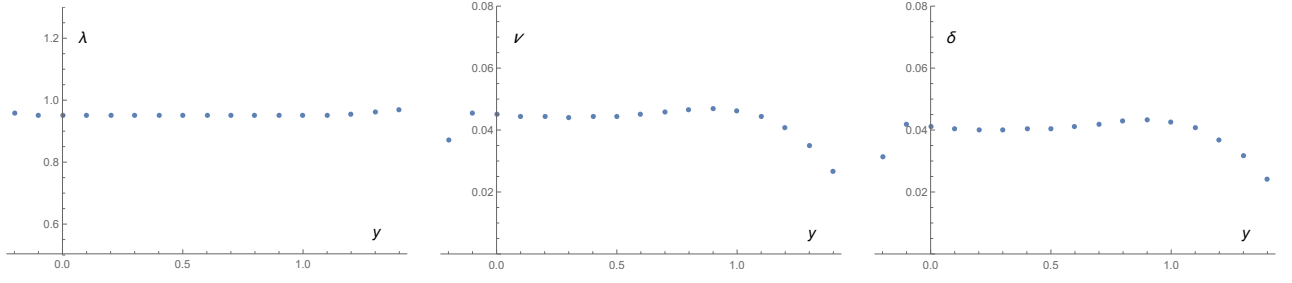


FIG. 6: Dependencies of λ , ν , and the LT violation δ on the lepton-pair rapidity y for the COMPASS kinematics.

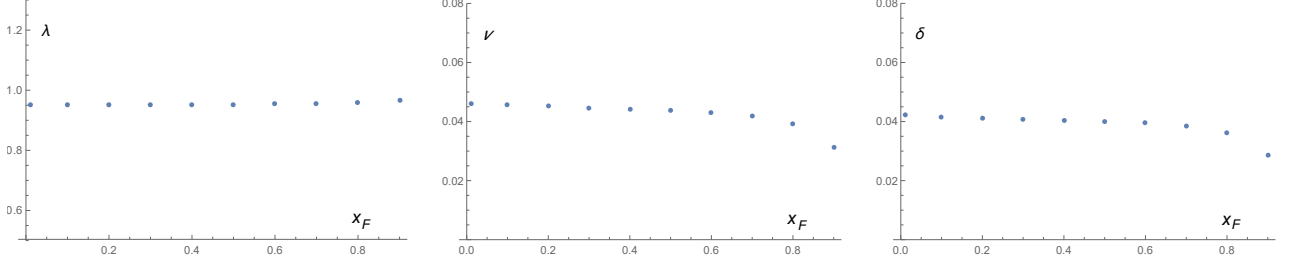


FIG. 7: Dependencies of λ , ν , and the LT violation δ on the Feynman variable x_F for the COMPASS kinematics.

The same Glauber phase also improves the agreement between the theoretical results and the COMPASS data for λ , ν and δ simultaneously.

We also present our predictions for the dependencies of λ , ν and δ on the lepton-pair rapidity y in Fig. 6 and on the Feynman variable x_F in Fig. 7 for the COMPASS kinematics. In the former case the definitions of the angular coefficients,

$$\lambda, \mu, \nu = \frac{\int dQ^2 dq_T^2 H_{\lambda, \mu, \nu}(Q^2, y, q_T^2)}{\int dQ^2 dq_T^2 H_0(Q^2, y, q_T^2)}, \quad (18)$$

are adopted, for which Eq. (17) can be converted into the allowed ranges of q_T and Q straightforwardly. In the latter case the set of variables Q , y and q_T has to be changed to the set of Q , y and x_F first. The phase space covers the full range of $q_T = [0.4, 3.0]$ GeV basically within $y = [-0.1, 1.1]$ ($x_F = [0, 0.7]$), explaining why stable regions exist in y (x_F) for λ , ν and δ as shown in Fig. 6 (Fig. 7). Since all the functions $H_i(Q^2, y, q_T^2)$ in Eq. (3) decrease with q_T as stated before, the contributions to the angular coefficients are dominated by $q_T < 1$ GeV. It is then easy to understand the value of λ about 0.95 and the small values of ν and δ around 0.04 in both figures, which are close to those for $q_T < 1$ GeV in Fig. 5. The quick descents of ν and δ near the high ends of y and x_F , where the range of q_T shrinks toward small q_T , also match the results in Fig. 5.

It is instructive to examine whether the angular coefficients modified by the Glauber effect obey the positivity constraints on the rotation-invariant observables [50, 51], which are defined in terms of the angular coefficients. Two SO(3) invariants survive in the present case with only virtual photon contributions [51],

$$U_2 = \frac{\lambda^2 + 3\mu^2 + 3\nu^2/4}{(3 + \lambda)^2}, \quad T = \frac{(\lambda + 3\nu/2)(2\lambda^2 + 9\mu^2 - 3\lambda\nu)}{(3 + \lambda)^3}. \quad (19)$$

To compute the angular coefficients in the above expressions, we integrate H_i in Eq. (3) over Q^2 , y and q_T^2 , and then take their ratios. Considering the NA10 kinematics for the pion beam energy $E_\pi = 194$ GeV, and performing the integration over the range of $q_T = [0, 2.5]$ GeV, we find that the values of μ and ν are quite small, and λ is close to unity. They thus lead to $U_2 = 0.062$ and $T = 0.031$, which satisfy the positivity constraints $U_2 \leq 1/4$ and $-1/8 \leq T \leq 3/8$ [51], respectively. In addition to the SO(3) invariants, one can consider the SO(2) invariants [51],

which are given, in terms of the same angular coefficients, by

$$\begin{aligned} I_x &= \frac{1 + \lambda - \nu}{3 + \lambda} = 0.498, & I_y &= \frac{1 + \lambda + \nu}{3 + \lambda} = 0.501, & I_z &= \frac{1 - \lambda}{3 + \lambda} = 0.002, \\ I_{xx} &= \frac{1}{4}(I_x - 1)^2 - \frac{(\lambda + \nu/2)^2}{(3 + \lambda)^2} = 0.001, & I_{yy} &= \frac{1}{4}(I_y - 1)^2 - \frac{(\lambda - \nu/2)^2 + 4\mu^2}{(3 + \lambda)^2} = 0.001, \\ I_{zz} &= \frac{1}{4}(I_z - 1)^2 - \frac{\nu^2}{(3 + \lambda)^2} = 0.249. \end{aligned} \quad (20)$$

The above results also respect the constraints $0 \leq I_x, I_y, I_z \leq 1$ and $0 \leq I_{xx}, I_{yy}, I_{zz} \leq 1/4$ [51].

In particular, I_y is identical to the invariant $\mathcal{F} = (1 + \lambda_0)/(3 + \lambda_0)$ introduced in [52] with the angular coefficient

$$\lambda_0 = \frac{\lambda + 3\nu/2}{1 - \nu/2}, \quad (21)$$

in the privileged frame [53]. The numerator and the denominator of λ_0 are expressed as the convolutions of the PDFs with the hard kernels

$$\left(\frac{E_1}{E_2} + \frac{E_2}{E_1} \right) \frac{1}{\sin^2 \theta_1} + \frac{(\cos S - 1)}{\sin^2 \theta_1} \left[\frac{E_1}{E_2} + \frac{E_2}{E_1} - 2 \left(\frac{E_1 E_2}{k^2} \sin^2 \theta_1 + 1 \right) \cos^2 \theta_1 \right], \quad (22)$$

and

$$\left(\frac{E_1}{E_2} + \frac{E_2}{E_1} \right) \frac{1}{\sin^2 \theta_1} - \frac{(\cos S - 1)}{\sin^2 \theta_1} \left(\frac{E_1 - 2k}{E_2} + \frac{E_2 - 2k}{E_1} - \frac{2E_1 E_2}{k^2} \cos^2 \theta_1 + 4 \right), \quad (23)$$

respectively. As expected, we recover $\lambda_0 = 1$ as the LT relation holds [53], i.e., as the Glauber phase S vanishes.

The geometric approach developed in [53–56] has provided a transparent illustration of how higher-order corrections in the perturbation theory give rise to the LT violation. The argument starts from the lepton pair production in a quark-anti-quark annihilation process, which obeys the angular distribution $1 + \cos^2 \theta_0$ with θ_0 being the polar angle of a lepton relative to one of the colliding quarks in the rest frame of the lepton pair [57]. Only when an on-shell quark and an on-shell anti-quark annihilate, does the produced lepton pairs obey this simple distribution. Therefore, the geometric picture applies better to the region with q_T being much lower than other hard scales like Q , in which the colliding quarks stay on-shell approximately after radiating collinear gluons. The angle θ_0 is then related to θ and ϕ in the CS frame through [54, 55]

$$\cos \theta_0 = \cos \theta \cos \theta_1 + \sin \theta \sin \theta_1 \cos(\phi - \phi_1), \quad (24)$$

with θ_1 (ϕ_1) being the polar (azimuthal) angle of the colliding quark referred to above in the CS frame. The angle θ_1 has the same meaning as that in Eq. (6), and $\phi_1 = 0$ at LO, i.e., for the $O(\alpha_s)$ diagrams in Fig. 1. The angular coefficients λ and ν are expressed in terms of θ_1 and ϕ_1 as

$$\lambda = \frac{2 - 3A_0}{2 + A_0}, \quad \nu = \frac{2A_2}{2 + A_0}, \quad (25)$$

with the functions $A_0 = \langle \sin^2 \theta_1 \rangle$ and $A_2 = \langle \sin^2 \theta_1 \cos(2\phi_1) \rangle$, where the averages are performed over an event sample, i.e., over the corresponding differential cross section.

As stated in [54], the dependence on the azimuthal angle ϕ_1 of the quark plane is caused by transverse momenta of radiative gluons, which can be achieved at $O(\alpha_s^2)$. Certainly, the values of θ_1 at $O(\alpha_s)$ and at $O(\alpha_s^2)$ may differ too, but this difference does not affect the reasoning below. The inequality $A_2 \leq A_0$ due to $\cos(2\phi_1) \leq 1$ then breaks the LT relation, yielding a negative violation δ . The predicted negative δ [30], contrary to the experimental indication of the pion-induced Drell-Yan processes at low q_T , hints that the LT violation might originate from a nonperturbative mechanism. The BM function, as a TMD PDF, invokes the correlation between the spin of the colliding quark and its transverse momentum, which modifies the perturbative results of ν , but not those of λ . Hence, it represents an additional contribution to the geometric picture, in which the colliding quarks are unpolarized. This is the reason why the BM mechanism can stimulate a positive δ at $O(\alpha_s^0)$ by breaking the azimuthal symmetry of the lepton pair distribution, that fits the data of the pion-induced Drell-Yan processes. Note that the sign of δ is not a prediction of the BM proposal, but a fit from the data.

The Glauber gluon effect on the LO results, different from the above known contributions, can also be elaborated in terms of the geometric picture. The necessary rung gluon emission on the pion side in Fig. 1(a), being mainly collinear,

tends to decrease the anti-quark energy and to lower the lepton-pair invariant mass Q . The azimuthal angle ϕ_1 of the quark plane remains tiny under the collinear gluon emission. For a given q_T , it implies that the mechanism tends to enlarge θ_1 , and thus decreases the coefficient λ and increases ν in Eq. (25). A Glauber gluon then injects a transverse momentum into the colliding quarks, rendering them off-shell and space-like. The produced lepton pairs will follow a modified angular distribution $\epsilon + \cos^2 \theta_0$ with the parameter $\epsilon < 1$ being attributed to the space-like virtuality of the quarks. This modified distribution can be derived trivially by computing the differential cross section for the annihilation $\bar{q} + q \rightarrow \ell^- + \ell^+$ with off-shell initial quarks. The insertion of Eq. (24) leads to a smaller denominator $2\epsilon + A_0$ in Eq. (25), such that the net effect makes a minor impact on λ , but a strong enhancement of ν . The above simple reasoning elucidates the results in Fig. 2, and the positive deviations δ derived in our analysis. We remark that both nontrivial ϵ and ϕ_1 can be induced at $O(\alpha_s^2)$ for high q_T in the geometric approach, and this complicated case deserves a thorough discussion.

In this paper we have demonstrated that the Glauber gluon effect, having been employed to resolve the several puzzles in the heavy quark decays, can explain the violation of the LT relation in the pion-induced Drell-Yan processes. The Glauber phase $S \sim 0.8$ is the only free parameter in our formalism, which was fixed by the NA10 data for the angular coefficient ν with a higher precision. This phase was then used to predict the coefficient λ and the LT violation $2\nu + \lambda - 1$, which were shown to accommodate all the data from the NA10, E615 and COMPASS experiments. Compared to the previous study, we have adopted the realistic PDFs for a proton from the CT18 and for a pion from the xFitter, included the QCD evolutions of the strong coupling and the PDFs, and integrated the differential cross section over the kinematic region considered in the above measurements. We have argued that the Glauber effect may be significant in pion-induced processes due to the unique role of a pion as a NG boson and a $q\bar{q}$ bound state, and illustrated it in the geometric picture. The distinctions from the perturbative and BM mechanisms have been stressed, and measuring the lepton pair distribution in the proton-anti-proton Drell-Yan process at low q_T can discriminate the different resolutions for the LT violation. Precise data of the coefficient λ can also serve the purpose, for which the perturbative and BM results stay below those from the Glauber effect. It is mentioned that the angular distribution of the lepton pairs in the proton-anti-proton Drell-Yan process produced at the Z pole by the CDF [58] satisfies the LT relation in the lowest bin of $q_T = 0\text{--}10$ GeV. It will be an important measurement [59] for exploring the internal structures of hadrons and for understanding the correlation of colliding partons in Drell-Yan processes. If the Glauber effect associated with a pion turns out to be crucial, it should be included in the extraction of the TMD pion PDF from the data of pion induced Drell-Yan processes.

Acknowledgments

We thank W.C. Chang, T.J. Hou, Y.S. Lian, and J.C. Peng for useful discussions. This work was supported by the National Science Council of R.O.C. under the Grant No. NSC-101-2112-M-001-006-MY3.

Appendix A: Average Glauber Phase

In this Appendix we explain how to take the average of the Glauber phase S for Figs. 1(a) and 1(b), and how this operation simplifies the corresponding factorization formulas. We quote Eq. (29) of Ref. [39] for the factorization of one Glauber gluon exchange on the left-hand side of the final-state cut in Fig. 1(a),

$$T_L^{(1)} \approx -i \frac{g^2}{(2\pi)^2} \int \frac{d^2 l_T}{l_T^2 + m_g^2} H(\mathbf{p}_{1T} - \mathbf{l}_T - \mathbf{q}_T, \mathbf{p}_{1T} - \mathbf{q}_T) \Phi_\pi(\mathbf{p}_{1T} - \mathbf{l}_T, \mathbf{p}_{1T}) \cdots, \quad (\text{A1})$$

where the kinematic variables have been modified to coincide with those in this work, and \cdots represents other factors not explicitly shown. The first argument of the hard kernel H (the TMD pion PDF Φ_π) denotes the transverse momentum of the virtual (valence) quark on the left-hand side of the final-state cut, and the second arguments denote those on the right-hand side of the cut. Equation (A1) indicates that the transverse momentum l_T of the Glauber gluon flows through the hard kernel H , and that an infrared divergence is generated from the region $l_T \rightarrow 0$ to be regularized by a gluon mass m_g . The intrinsic transverse momentum p_{1T} in the pion is small, and lower than 1 GeV typically. Since the lepton-pair transverse momentum q_T is about few GeV, at which the LT violation is significant, the integrals over l_T and p_{1T} in the dominant Glauber region depend on q_T weakly.

We then apply the approximation $H(\mathbf{p}_{1T} - \mathbf{l}_T - \mathbf{q}_T, \mathbf{p}_{1T} - \mathbf{q}_T) \approx H(\mathbf{q}_T)$ by neglecting the smaller l_T and p_{1T} , and Fourier transform Eq. (A1) into the impact-parameter space,

$$T_L^{(1)} \approx \int d^2 b_l d^2 b_r \Phi_\pi(\mathbf{b}_l, \mathbf{b}_r) [-iS(\mathbf{b}_l)] H(\mathbf{q}_T) e^{i\mathbf{p}_{1T} \cdot (\mathbf{b}_l - \mathbf{b}_r)} \cdots, \quad (\text{A2})$$

with the one-loop Glauber factor [39]

$$S(\mathbf{b}) = \frac{g^2}{(2\pi)^2} \int \frac{d^2 l_T}{l_T^2 + m_g^2} e^{-i\mathbf{l}_T \cdot \mathbf{b}} = \frac{g^2}{2\pi} K_0(bm_g), \quad (\text{A3})$$

K_0 being the modified Bessel function. Because the two virtual quarks carry the same transverse momentum under the approximation, a single argument \mathbf{q}_T for H is enough. The addition of one Glauber gluon to the right-hand side of the final-state cut, and the extension of the factorization for Glauber gluons to all orders lead to

$$\begin{aligned} \frac{d\sigma}{dQ^2 dy dq_T^2 d\Omega} &\approx \int d^2 b_l d^2 b_r \int \frac{d^2 k_{3T}}{(2\pi)^2} \Phi_\pi(\mathbf{b}_l, \mathbf{b}_r) e^{-iS(\mathbf{b}_l)} H(\mathbf{q}_T) e^{iS(\mathbf{b}_r)} \\ &\times \Phi_p(\mathbf{b}_l - \mathbf{b}_r) e^{i(\mathbf{q}_T + \mathbf{k}_{3T}) \cdot (\mathbf{b}_l - \mathbf{b}_r)}, \end{aligned} \quad (\text{A4})$$

which can be deduced straightforwardly by following the steps in Sec. III of Ref [39]. Briefly speaking, the δ function $\delta^2(\mathbf{p}_{1T} + \mathbf{p}_{2T} - \mathbf{q}_T - \mathbf{k}_{3T})$ for the momentum conservation is integrated over p_{1T} , such that $e^{i\mathbf{p}_{1T} \cdot (\mathbf{b}_l - \mathbf{b}_r)}$ in Eq. (A1) produces two Fourier factors $e^{-i\mathbf{p}_{2T} \cdot (\mathbf{b}_l - \mathbf{b}_r)}$ and $e^{i(\mathbf{q}_T + \mathbf{k}_{3T}) \cdot (\mathbf{b}_l - \mathbf{b}_r)}$. The former brings the TMD proton PDF Φ_p into the impact-parameter space after the integration over p_{2T} , giving $\Phi_p(\mathbf{b}_l - \mathbf{b}_r)$. The latter has been kept in Eq. (A4).

The Fourier factor $e^{i(\mathbf{q}_T + \mathbf{k}_{3T}) \cdot (\mathbf{b}_l - \mathbf{b}_r)}$ does not vary much with $\mathbf{b}_l - \mathbf{b}_r$ in the region governed by the TMD proton PDF, for $\mathbf{q}_T + \mathbf{k}_{3T}$ is as small as the intrinsic transverse momenta. This insensitivity allows the introduction of a constant Glauber factor $e^{iS} \equiv \langle e^{i[S(\mathbf{b}_r) - S(\mathbf{b}_l)]} \rangle$, which is computed as an average over the impact parameters b_l and b_r . Noticing that only the real part $\cos S$ contributes to the differential cross section, we rewrite Eq. (A4) as

$$\frac{d\sigma}{dQ^2 dy dq_T^2 d\Omega} \approx \cos S \int d^2 b_l d^2 b_r \int \frac{d^2 k_{3T}}{(2\pi)^2} \Phi_\pi(\mathbf{b}_l, \mathbf{b}_r) H(\mathbf{q}_T) \Phi_p(\mathbf{b}_l - \mathbf{b}_r) e^{i(\mathbf{q}_T + \mathbf{k}_{3T}) \cdot (\mathbf{b}_l - \mathbf{b}_r)}. \quad (\text{A5})$$

The integration of $e^{i\mathbf{k}_{3T} \cdot (\mathbf{b}_l - \mathbf{b}_r)}$ over k_{3T} yields $(2\pi)^2 \delta^2(\mathbf{b}_l - \mathbf{b}_r)$, which is then integrated over b_l to arrive at $e^{i\mathbf{q}_T \cdot (\mathbf{b}_l - \mathbf{b}_r)} = 1$ and $\Phi_p(\mathbf{b}_l - \mathbf{b}_r = 0) = \phi_p$, i.e., the proton PDF appearing in Eq. (4). At last, Eq. (40) in Ref. [39], i.e., $\int d^2 b_r \Phi_\pi(\mathbf{b}_r, \mathbf{b}_r) = \phi_\pi$, which relates a two-parameter PDF to the corresponding standard PDF, is implemented, and Eq. (A5) reduces to the factorization formula in Eq. (4).

For the addition of Glauber gluons to Fig. 1(b), we simply replace $H(\mathbf{q}_T)$ in Eq. (A2) by $H(\mathbf{k}_{3T})$, and Eq. (A5) becomes

$$\frac{d\sigma}{dQ^2 dy dq_T^2 d\Omega} \approx \cos S \int d^2 b_l d^2 b_r \int \frac{d^2 k_{3T}}{(2\pi)^2} \Phi_\pi(\mathbf{b}_l, \mathbf{b}_r) H(\mathbf{k}_{3T}) \Phi_p(\mathbf{b}_l - \mathbf{b}_r) e^{i(\mathbf{q}_T + \mathbf{k}_{3T}) \cdot (\mathbf{b}_l - \mathbf{b}_r)}. \quad (\text{A6})$$

The integration over k_{3T} then transforms $H(\mathbf{k}_{3T})$ into $H(\mathbf{b}_l - \mathbf{b}_r)$ in the impact-parameter space. The large scale in the hard kernel, being of order of Q , requires $\mathbf{b}_l \approx \mathbf{b}_r$, such that $\Phi_\pi(\mathbf{b}_l, \mathbf{b}_r) \approx \Phi_\pi(\mathbf{b}_r, \mathbf{b}_r)$ and $\Phi_p(\mathbf{b}_l - \mathbf{b}_r \approx 0) \approx \phi_p$. The variable change $\mathbf{b}'_l = \mathbf{b}_l - \mathbf{b}_r$ and the integration of $H(\mathbf{b}'_l) e^{i\mathbf{q}_T \cdot \mathbf{b}'_l}$ over \mathbf{b}'_l return $H(\mathbf{q}_T)$. At last, the integration of $\Phi_\pi(\mathbf{b}_r, \mathbf{b}_r)$ over b_r gives ϕ_π , and we are again led to the factorization formula in Eq. (4).

-
- [1] R. J. Oakes, *Nuovo Cimento* **44A**, 440 (1966).
 - [2] C. S. Lam and W. K. Tung, *Phys. Rev. D* **18**, 2447 (1978); *Phys. Rev. D* **21**, 2712 (1980).
 - [3] J. C. Collins and D. E. Soper, *Phys. Rev. D* **16**, 2219 (1977).
 - [4] E. Mirkes, *Nucl. Phys.* **B387**, 3 (1992); E. Mirkes and J. Ohnemus, *Phys. Rev. D* **51**, 4891 (1995).
 - [5] E. L. Berger, J. W. Qiu, and R. A. Rodriguez-Pedraza, *Phys. Lett. B* **656**, 74 (2007); *Phys. Rev. D* **76**, 074006 (2007).
 - [6] J. Cleymans and M. Kuroda, *Phys. Lett.* **105B**, 68 (1981).
 - [7] P. Chiappetta and M. Le Bellac, *Z. Phys. C* **32**, 521 (1986).
 - [8] L. Y. Zhu *et al.* (E866/NuSea Collaboration), *Phys. Rev. Lett.* **99**, 082301 (2007); *Phys. Rev. Lett.* **102**, 182001 (2009).
 - [9] S. Falciano *et al.* (NA10 Collaboration), *Z. Phys. C* **31**, 513 (1986); M. Guanziroli *et al.* (NA10 Collaboration), *Z. Phys. C* **37**, 545 (1988).
 - [10] J. S. Conway *et al.*, *Phys. Rev. D* **39**, 92 (1989); J.G. Heinrich *et al.*, *Phys. Rev. D* **44**, 1909 (1991).
 - [11] Y. H. Lien and A. Chumakov, in *Proceedings of the XXVIII International Workshop on Deep-Inelastic Scattering and Related Subjects* (Stony Brook University, New York, 2021).
 - [12] A. Brandenburg, O. Nachtmann, and E. Mirkes, *Z. Phys. C* **60**, 697 (1993).
 - [13] D. Boer, A. Brandenburg, O. Nachtmann, and A. Utermann, *Eur. Phys. J. C* **40**, 55 (2005).
 - [14] A. Brandenburg, S. J. Brodsky, V. V. Khoze and D. Muller, *Phys. Rev. Lett.* **73**, 939 (1994).
 - [15] K. J. Eskola, P. Hoyer, M. Vanttinen and R. Vogt, *Phys. Lett. B* **333**, 526 (1994).

- [16] D. Boer and P. J. Mulders, Phys. Rev. D **57**, 5780 (1998); D. Boer, Phys. Rev. D **60**, 014012 (1999).
- [17] D. Boer, S. J. Brodsky and D. S. Hwang, Phys. Rev. D **67**, 054003 (2003).
- [18] Z. Lu and B. Q. Ma, Phys. Rev. D **70**, 094044 (2004); Phys. Lett. B **615**, 200 (2005).
- [19] D. Boer, A. Brandenburg, O. Nachtmann, and A. Utermann, Eur. Phys. J. C **40**, 55 (2005).
- [20] L. P. Gamberg and G. R. Goldstein, Phys. Lett. B **650**, 362 (2007).
- [21] C. p. Chang and H. n. Li, Phys. Lett. B **726**, 262 (2013).
- [22] J. Zhou, F. Yuan and Z. T. Liang, Phys. Lett. B **678**, 264 (2009).
- [23] Z. Lu and I. Schmidt, Phys. Rev. D **81**, 034023 (2010); V. Barone, S. Melis, and A. Prokudin, Phys. Rev. D **82**, 114025 (2010).
- [24] J. Collins and J. W. Qiu, Phys. Rev. D **75**, 114014 (2007).
- [25] J. Collins, arXiv:0708.4410 [hep-ph].
- [26] G. P. Lepage and S. J. Brodsky, Phys. Lett. B **87**, 359 (1979); S. Nussinov and R. Shrock, Phys. Rev. D **79**, 016005 (2009).
- [27] T. J. Hou, J. Gao, T. J. Hobbs, K. Xie, S. Dulat, M. Guzzi, J. Huston, P. Nadolsky, J. Pumplin, C. Schmidt *et al.* Phys. Rev. D **103**, 014013 (2021).
- [28] I. Novikov, H. Abdolmaleki, D. Britzger, A. Cooper-Sarkar, F. Giuli, A. Glazov, A. Kusina, A. Luszczak, F. Olness and P. Starovoitov, *et al.* Phys. Rev. D **102**, no.1, 014040 (2020).
- [29] P. C. Barry, N. Sato, W. Melnitchouk and C. R. Ji, Phys. Rev. Lett. **121**, 152001 (2018).
- [30] W. C. Chang, R. E. McClellan, J. C. Peng and O. Teryaev, Phys. Rev. D **99**, 014032 (2019).
- [31] W. C. Chang, R. E. McClellan, J. C. Peng and O. Teryaev, Proc. Sci. DIS2019 (2019) 172 [arXiv:1907.11356 [hep-ph]].
- [32] M. Lambertsens and W. Vogelsang, Phys. Rev. D **93**, 114013 (2016).
- [33] D. Boer and W. Vogelsang, Phys. Rev. D **74**, 014004 (2006).
- [34] K. Kajantie, J. Lindfors, and R. Raitio, Phys. Lett. **74B**, 384 (1978).
- [35] C. S. Lam and W. K. Tung, Phys. Lett. **80B**, 228 (1979).
- [36] J. C. Collins, Phys. Rev. Lett. **42**, 291 (1979).
- [37] J. Cleymans and M. Kuroda, Nucl. Phys. **B155**, 480 (1979); **B160**, 510(E) (1979)].
- [38] J. Lindfors, Phys. Scr. **20**, 19 (1979).
- [39] C. p. Chang and H. n. Li, Eur. Phys. J. C **71**, 1687 (2011); H.-n. Li, arXiv:1009.3610 [hep-ph].
- [40] X. Liu, H. n. Li and Z. J. Xiao, Phys. Rev. D **91**, 114019 (2015).
- [41] S. Mishima and H. n. Li, Phys. Rev. D **73**, 114014 (2006).
- [42] H. n. Li and S. Mishima, Phys. Rev. D **83**, 034023 (2011).
- [43] H. n. Li and S. Mishima, Phys. Rev. D **90**, 074018 (2014).
- [44] H. n. Li, S. Mishima, and A. I. Sanda, Phys. Rev. D **72**, 114005 (2005).
- [45] X. Liu, H. n. Li and Z. J. Xiao, Phys. Rev. D **93**, 014024 (2016).
- [46] H. Y. Cheng and C. W. Chiang, Phys. Rev. D **81**, 074021 (2010).
- [47] H. n. Li, C. D. Lu, and F. S. Yu, Phys. Rev. D **86**, 036012 (2012).
- [48] H. n. Li, Chin. J. Phys. **73**, 649 (2021).
- [49] V. Khachatryan *et al.* (CMS Collaboration), Phys. Lett. B **750**, 154 (2015).
- [50] Y. Q. Ma, J. W. Qiu and H. Zhang, arXiv:1703.04752 [hep-ph].
- [51] M. Gavriloa and O. Teryaev, Phys. Rev. D **99**, 076013 (2019).
- [52] P. Faccioli, C. Lourenco and J. Seixas, Phys. Rev. Lett. **105**, 061601 (2010).
- [53] O. V. Teryaev, in Proceedings of the XI Advanced Research Workshop on High Energy Spin Physics, pp. 171–175 (Dubna, 2005) [arXiv:2012.11720 [hep-ph]].
- [54] J. C. Peng, W. C. Chang, R. E. McClellan, and O. Teryaev, Phys. Lett. B **758**, 384 (2016).
- [55] W. C. Chang, R. E. McClellan, J. C. Peng and O. Teryaev, Phys. Rev. D **96**, 054020 (2017).
- [56] J. C. Peng, D. Boer, W. C. Chang, R. E. McClellan and O. Teryaev, Phys. Lett. B **789**, 356 (2019).
- [57] P. Faccioli, C. Lourenco, J. Seixas, and H. Wohri, Phys. Rev. D **83**, 056008 (2011).
- [58] T. Aaltonen *et al.* (CDF Collaboration), Phys. Rev. Lett. **106**, 241801 (2011).
- [59] L. Frankfurt, M. Strikman, A. Larionov, A. Lehrach, R. Maier, H. van Hees, C. Spieles, V. Vovchenko and H. Stöcker, arXiv:1808.09550 [hep-ph].